PROGRESS IN PHOTOVOLTAICS: RESEARCH AND APPLICATIONS
Prog. Photovolt: Res. Appl. (2012)
Published online in Wiley Online Library (wileyonlinelibrary.com). DOI: 10.1002/pip.2154

RESEARCH ARTICLE

Multi-pronged analysis of degradation rates of photovoltaic modules and arrays deployed in Florida

K. O. Davis[1]*, S. R. Kurtz[2], D. C. Jordan[2], J. H. Wohlgemuth[2] and N. Sorloaica-Hickman[1]*

[1] Florida Solar Energy Center, University of Central Florida, 1679 Clearlake Rd., Cocoa, FL 32922–5703, USA
[2] National Renewable Energy Laboratory, 1617 Cole Blvd., Golden, CO 80401–3305, USA

ABSTRACT

The long-term performance and reliability of photovoltaic (PV) modules and systems are critical metrics for the economic viability of PV as a power source. In this study, the power degradation rates of two identical PV systems deployed in Florida are quantified using the Performance Ratio analytical technique and the translation of power output to an alternative reporting condition of 1000 W m^{-2} irradiance and cell temperature of 50 °C. We introduce a multi-pronged strategy for quantifying the degradation rates of PV modules and arrays using archived data. This multi-pronged approach utilizes nearby weather stations to validate and, if needed, correct suspect environmental data that can be a problem when sensor calibrations may have drifted. Recent field measurements, including *I-V* curve measurements of the arrays, visual inspection, and infrared imaging, are then used to further investigate the performance of these systems. Finally, the degradation rates and calculated uncertainties are reported for both systems using the methods described previously.

KEYWORDS

degradation rate; energy yield; archived data; Performance Ratio

***Correspondence**

Kristopher Davis, Nicoleta Sorloaica-Hickman, Florida Solar Energy Center, 1679 Clearlake Rd., Cocoa, FL 32922–5703, USA.
E-mail: kdavis@fsec.ucf.edu; nhickman@fsec.ucf.edu

Received 24 June 2011; Revised 27 November 2011; Accepted 30 November 2011

1. INTRODUCTION

Field testing has played a vital part in determining photovoltaic (PV) performance and lifetime. Dating back to 1983, the Florida Solar Energy Center (FSEC) has performed outdoor performance measurements on various kinds of PV modules at different locations in Florida, as shown in Figure 1. With over 150 systems listed in the FSEC PV system database, 70 of which have performance data, there is clearly a rich history of archived data that can be used to better understand and quantify the long-term performance of PV modules and systems. DC operating current, DC operating voltage, and AC power were recorded for extended periods of time (greater than 3 years), along with environmental conditions such as plane-of-array (POA) irradiance, module temperature, and ambient temperature.

For many of these systems, the initial data monitoring served some function other than determining long-term performance degradation. Some of the systems were used to better understand the role of PV in the development of zero-energy buildings [1,2]. Other PV systems, installed on schools in Florida, were monitored to educate students on PV technology and also gather statistical information regarding life-cycle costs [3]. Recent efforts have sought to relate the long-term performance of these systems to life-cycle costs and economic payback time [4].

Long-term performance of PV systems is an area of critical importance from the perspective of both manufacturers and end users. End users want to harvest the maximum amount of energy per rated watt throughout the expected 20+ year operational lifetime. To stay competitive, module manufacturers guarantee minimal degradation throughout the lifetime of the product. Standard warranties typically guarantee a power output after 20 years of 80% of Standard Test Conditions (STC) nameplate. Clearly, if a large number of a manufacturer's modules have higher degradation rates than expected, then the company's financial security can be significantly compromised by the cost of replacing these defective products. There is also potential damage to a

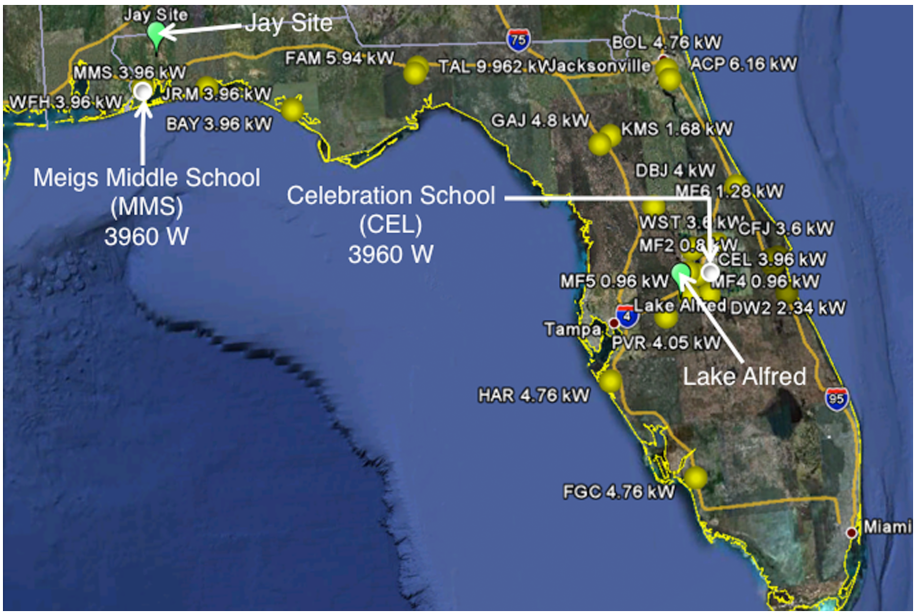

Figure 1. Locations of the two photovoltaic (PV) systems investigated in this study, their nearby weather stations, and additional PV sites monitored by Florida Solar Energy Center.

company's reputation if durability becomes a perceived issue with their products.

The study of degradation rates is often challenging because confidence in the results increases with the number of years of data collected from the field, but it is uncommon for projects to be consistently funded for more than a small number of years. The result is a collection of a few excellent studies and many more studies that report data with higher uncertainties [5–17].

In this investigation, experimental data from two nominally identical grid-connected PV systems (Figure 1) were analyzed in order to evaluate performance and reliability, with a focus on module power output over time. First, the systems, data collection, and data analysis methods are described. Then, the calculated degradation rates are presented along with the uncertainty associated with those degradation rates. Finally, observations from the field and results of on-site *I-V* measurements are discussed. This study introduces a multi-pronged analytical methodology to address some of the difficulties of accurately determining degradation rates of PV systems that have not been consistently maintained.

2. EXPERIMENTAL DETAILS

2.1. Description of the PV systems

Table I lists essential information about the systems under investigation, including system location, system size, module technology, date of installation, data collection period, and array configuration. These systems share virtually identical electrical designs, including the same size, modules, and inverters. Both systems are broken up into two sub-arrays (1.98 kW each) feeding two separate inverters, which were all 2.5 kW nominally rated.

2.2. Technical description of the instrumentation and monitoring method

For the system data monitoring, pyranometers were used to measure POA irradiance, thermocouples to measure ambient and back-of-module temperature, and different electrical sensors for DC current and voltage as well as AC energy output. Campbell Scientific dataloggers were used to sample these measured parameters at 5-s intervals, which were then averaged over 15 min and stored. This

Table I. Description of systems under investigation.

System location	System name	Array size (watts)	Module technology	Date of installation	Monitoring period	Array configuration
Shalimar, FL (latitude: 30°N)	Meigs Middle School	3960	polycrystalline-Si	February 2003	5.5 years	Mounted on flat roof at a 17° tilt
Celebration, FL (latitude: 28°N)	Celebration School	3960	polycrystalline-Si	December 2003	4 years	Mounted parallel to pitched roof at 15° tilt

method is based on techniques described in IEC 61724, a standard for monitoring PV system performance [18].

2.3. Data filtering and evaluation of data quality

Filtering steps were taken to minimize the effects of errors in data collection and measurement (e.g., instrument failure, faulty network communications). After experimenting with various filtering techniques, the process outlined in Figure 2 was chosen for this study. Plotting the collected parameters versus time is a good way to spot obvious errors in data collection. There are some specific things to look for that might not be obvious from the initial plots. These include the following: (i) irradiance sensor drift, which can be identified by plotting POA irradiance versus time (Figure 3); (ii) DC-to-AC conversion efficiency, which can be determined by plotting the ratio of AC power to DC power versus time (Figure 2); and (iii) plot V_{DC} versus time to see if the DC voltage is pinned to either the high or low window of the inverter's DC voltage range. This last check can identify low energy yield caused by improper maximum power-point tracking. If using the data to quantify degradation rates, then one final filtering step should be to only use data that starts and ends at the same time of the year (to avoid seasonal effects). After performing filtering, the two analytical techniques mentioned previously (power output translated to alternative reporting condition (ARC) and Performance Ratio (PR)) were used to analyze the experimental data collected for this study.

2.4. Effects of sensor drift and potential methods of correction

One common issue with using data collected over long periods of time at remote sites occurs when measurement instrumentation has not been consistently calibrated. When this happens, the data can be severely affected—especially in the case of pyranometers. Because of the approximately linear relationship between irradiance and current (and therefore power), sensor drift can drastically make the module degradation rate appear to be significantly higher or lower than it actually is. There are a number of ways to combat the effects of sensor drift. One method is to only use archived data for the first calibrated year, and then later either collect on-site measurements (e.g., *I-V* curves on the array) or recalibrate/replace the measurement instruments and begin collecting again remotely. The obvious downside to this method is that all of the data collected after year one gets neglected, leading to large gaps of time missing from the analysis and thereby significantly reducing the utility of the data set. In addition, with this method different instruments are used to measure the performance at different points of time.

Instead, another option is to correlate data measured with calibrated instruments taken at nearby sites and use that data to correct the data that has drifted. The primary limitation of this method is that it requires data collection

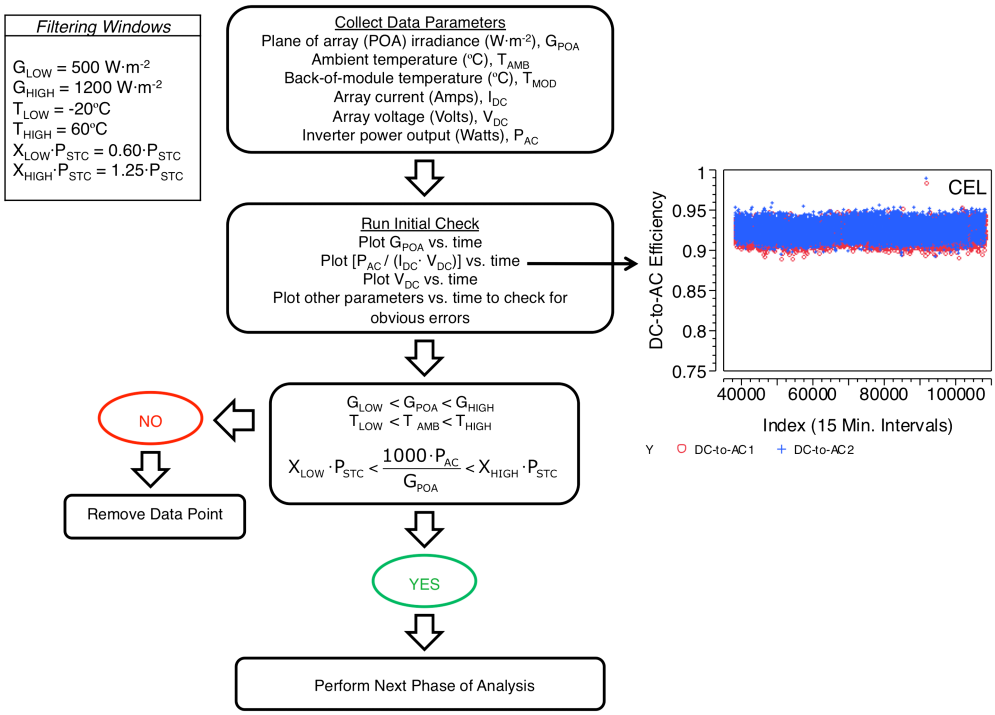

Figure 2. Initial data filtering process used to minimize errors.

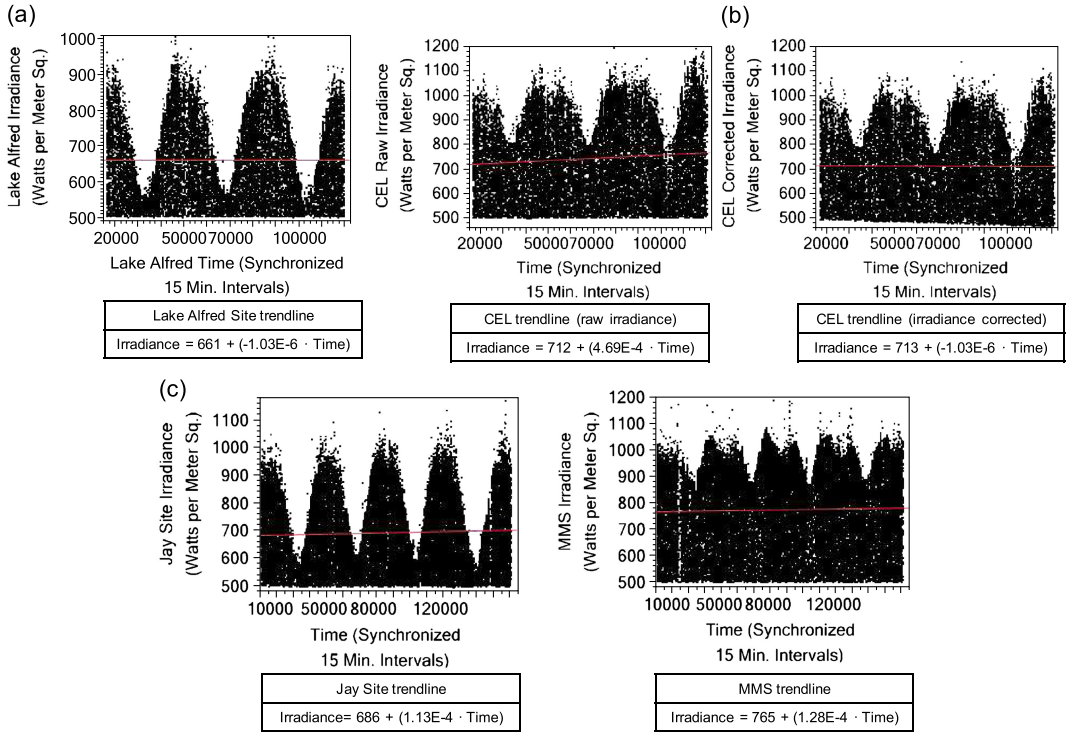

Figure 3. Comparison of site data and nearby weather stations: (a) Comparison of uncalibrated Celebration School (CEL) pyranometer and calibrated pyranometer installed nearby (Lake Alfred Site), (b) CEL pyranometer data corrected to match the trend line of the calibrated pyranometer data (Lake Alfred Site), (c) Comparison of uncalibrated Meigs Middle School (MMS) pyranometer and calibrated pyranometer installed at a nearby location (Jay Site).

from a nearby site, which can be difficult to come by. Luckily, thanks to the Florida Automated Weather Network (FAWN), administered by the University of Florida, 35 weather stations in Florida collect irradiance data. Figure 3 shows the original pyranometer data from the Celebration School (CEL) system (which shows obvious drift), data collected from a pyranometer at a nearby FAWN weather station, and the irradiance-corrected CEL data. The FAWN pyranometer, installed at a 0º tilt, is simply used to establish the trend line of irradiance over time for that local geographic region using a linear regression. A linear time-varying correction factor is then applied to the original irradiance data to establish a similar trend line, which provides the offset required to essentially eliminate the effects of sensor drift. This correction factor is applied by adding a linear time-varying term, $\Delta G = \kappa t \cdot (G_{\text{POA-raw}}/1000)$, to the raw irradiance data. ΔG is proportional to time (t), which is given as an index of the synchronized 15 min intervals, and κ, a constant that is determined empirically by comparing the slope of the corrected G_{POA} trend line to that of the nearby calibrated site. κ, and therefore ΔG, can be either positive or negative depending on which direction the sensor is drifting.

Figure 3 also shows the Meigs Middle School (MMS) pyranometer data alongside calibrated pyranometer data from a FAWN station close to the MMS site (also at 0º tilt). Here there is a close match in the irradiance trend line between the data sets, so no correction of irradiance was made. Conveniently, all data sets shared the 15-min averaging format, and a MATLAB program was written to assign an appropriate index number to each 15-min interval, which provided appropriate time synchronization for the data sets being compared.

2.5. Translating archived performance data to alternative reporting conditions

With regards to the archived data sets, the following well-established translation equations were used to correct the array and system power output measured over multiple years to an ARC, wherein the measured operating voltage ($V_{\text{MP-m}}$) is translated to 50 °C using the measured cell operating temperature (derived from the module's measured back-surface temperature) and measured operating current ($I_{\text{MP-m}}$) is translated to 1000 W m^{-2} using (corrected) measured incident POA irradiance and cell operating temperature.

$$V_{\text{MP-ARC}} = V_{\text{MP-m}} + TC_{\text{VMP}}(T_{\text{ARC}} - T_{\text{cell}}) \quad (1)$$

$$I_{\text{MP-ARC}} = I_{\text{MP-m}}\left(\frac{G_{\text{ARC}}}{G_{\text{POA}}}\right) + TC_{\text{IMP}}(T_{\text{ARC}} - T_{\text{cell}}) \quad (2)$$

$$P_{\text{MP-ARC}} = V_{\text{MP-ARC}} \cdot I_{\text{MP-ARC}} \quad (3)$$

Here, G_{POA} is again the (corrected) measured POA irradiance, and G_{ARC} is the reference irradiance (1000 W m^{-2}).

T_{ARC} is the cell temperature for the chosen set of reporting conditions (50 °C), and T_{cell} is the measured cell operating temperature, which is derived from the module's measured back-surface temperature using Equation (4) [19].

$$T_{cell} = T_m + \Delta T\left(\frac{G_{POA}}{G_{STC}}\right) \quad (4)$$

Because cell temperatures were measured using thermocouples attached to the backsheet of the modules (T_m), a small temperature correction factor should be applied to the back-of-module temperature values. ΔT represents the higher operating temperature of a cell compared with the module backsheet at an irradiance equal to G_{STC}. In this case, ΔT was taken to be 2.5 °C, which is a recommended value found in the literature [20,21].

Temperature coefficients for operating voltage (TC_{VMP}, given in units *V*/°C in Equation (1)) and operating current (TC_{IMP}, given in *A*/°C) were established by a linear regression on each sub-array, with voltage and irradiance-translated current as the response variables and module temperature the predictor. The slope of each regression was taken as the temperature coefficient for that sub-array, as seen graphically in Figure 4.

Once the temperature coefficients for each sub-array were identified, translation of DC power to ARC was then carried out. The reason for not using STC as the reporting condition is to minimize potential error in translation, because typical cell operating temperatures are generally much higher than 25 °C (which is what STC calls for), especially with irradiance at or near 1000 W m^{-2}.

2.6. Performance Ratio analysis

The Performance Ratio is essentially a measure of the energy yield of a PV array or system divided by the theoretical output given from the nameplate power rating of the array (i.e., the sum of all of the modules' power ratings). Mathematically, it is calculated from the following parameters [22].

$$Y_f(\text{kWh/kW}) = \frac{E_{OUT}(\text{kWh})}{P_{STC}(\text{kW})} \quad (4)$$

$$Y_r(\text{hours}) = \frac{H_{POA}\left(\text{kWhm}^{-2}\right)}{G_{STC}\left(\text{kWm}^{-2}\right)} \quad (5)$$

E_{OUT} is defined as the energy output of the array or the entire system over a defined period of time (e.g., month, day, 15-min interval), and P_{STC} is the nameplate array power output at STC. Y_f is the final energy yield and is the actual energy output (E_{OUT}) divided by P_{STC}. H_{POA} is the measured solar energy per area incident on the array over the same defined period of time used in E_{OUT}. G_{STC} is again the reference irradiance used to rate the array (1000 W m^{-2}). Y_r is the reference yield, which is the ratio of H_{POA} to G_{STC}. Finally, *PR* is the ratio of the final system yield divided by the reference yield:

$$PR = \frac{Y_f}{Y_r} \quad (6)$$

2.7. Degradation rate uncertainty

As described earlier, a linear regression is used to determine the actual rate of degradation. In this case, the response variable is P_{MP-ARC}, PR_{DC}, or PR_{AC} and the regressor is time (15-min intervals for P_{MP-ARC} and months for monthly *PR*). The slope of the linear fit gives the degradation trend and the actual degradation rate can be determined from the following,

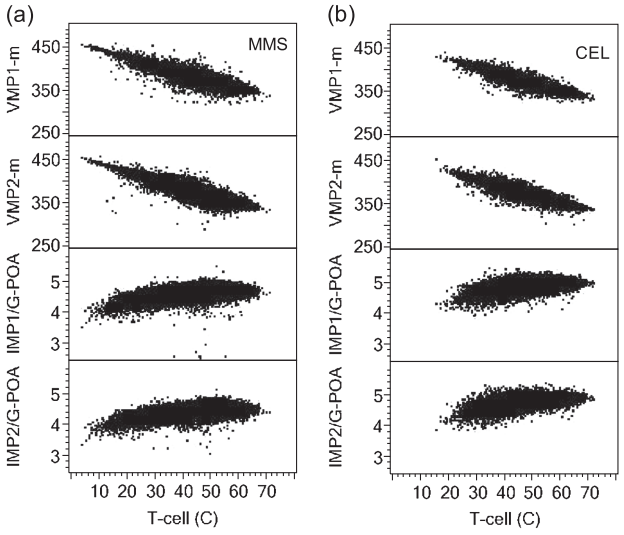

Sub-Array	TC_{VMP} (V/°C)	TC_{IMP} (A/°C)
MMS 1	-1.72	0.0071
MMS 2	-1.83	0.0071
CEL 1	-1.74	0.0084
CEL 2	-1.72	0.0087

Figure 4. Operating voltage and irradiance-translated operating current versus module temperature: (a) Meigs Middle School (MMS) data set; (b) irradiance-corrected Celebration School (CEL) data set; (c) temperature coefficients.

$$R_d = \frac{Na_1}{a_0} \tag{7}$$

where N is a multiplier to translate the degradation trend to the appropriate units of time (per year being the desired unit of time in this case), a_0 is the intercept, and a_1 is the slope. R_d is the degradation rate in units %/year, and is actually given as $R_d \pm \Delta R_d$. To calculate ΔR_d, the familiar sum of squares equation is used,

$$\Delta R_d = \sqrt{\left(\frac{\partial R_d}{\partial a_0}\right)^2 (\Delta a_0)^2 + \left(\frac{\partial R_d}{\partial a_1}\right)^2 (\Delta a_1)^2} \approx \left(\frac{N}{a_0}\right)(\Delta a_1) \tag{8}$$

The term with Δa_0 has minimal affect on ΔR_d and can therefore be neglected. The primary contribution comes from the slope uncertainty, Δa_1. To calculate Δa_1, a simple Type A evaluation has been carried out, which relies on statistical information of the sample to calculate the random uncertainty in the slope [23]. This method of calculating uncertainty fails to capture certain systematic uncertainties, which are primarily due to irradiance sensor drift. The aforementioned method of correcting sensor drift is meant to address this, but to fully understand this uncertainty contribution, a comprehensive Type B evaluation is needed [24]. This falls beyond the scope of this paper, but it is worth noting that the accuracy and calibration history of irradiance sensors appear to be the biggest hurdles in accurately quantifying degradation rates in PV systems. To better understand the impact of this issue, degradation rates were calculated for the CEL system with both the raw data and the irradiance-corrected data. The raw data was found to have 2%/year more degradation in both sub-arrays.

To summarize, the uncertainties reported in this paper are based only on the random uncertainty associated with the regression slope coefficient. These numbers could, and likely would, differ if systematic uncertainties were fully taken into account.

3. RESULTS AND DISCUSSION

3.1. Degradation rates based on P_{MP-ARC}

As the system performance changes over time, this translation to ARC provides a means of visualizing system performance over time (Figure 5) and quantifying the degradation rate of power output (see the first data column in Table II for the P_{MP-ARC} data; Table II gives a complete listing of all of the degradation rates discussed here). By performing a linear regression of the ARC-translated power for the MMS system, the calculated degradation rate for sub-array 1 was -0.84 ± 0.014%/year and -0.99 ± 0.013%/year for

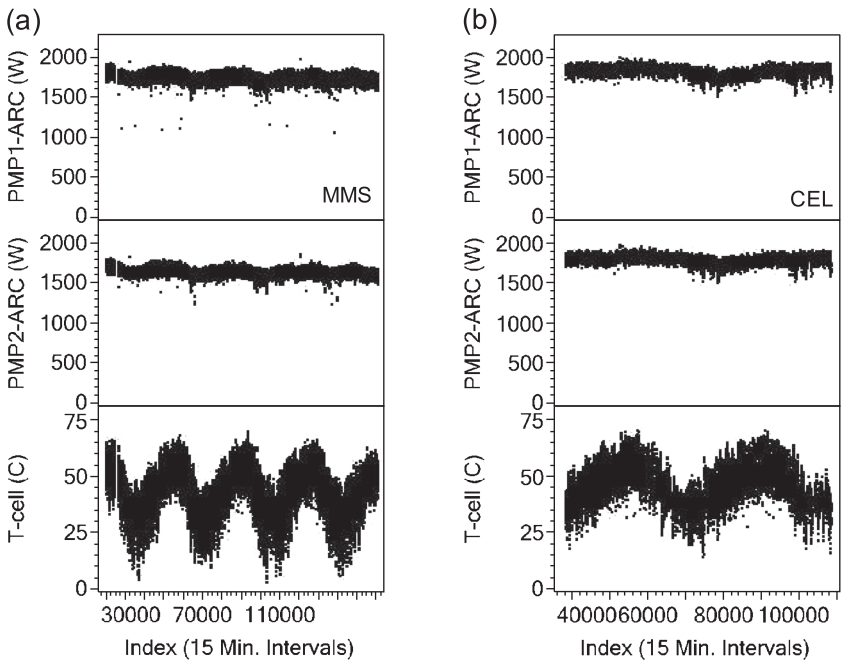

Figure 5. Array power output (alternative reporting condition (ARC)-translated) and module temperature versus time for: (a) Meigs Middle School (MMS) data set, (b) irradiance-corrected Celebration School (CEL) data set. The minor seasonal fluctuations occurring at data points with low temperatures are likely due to the uncertainty associated with the temperature measurements and temperature coefficients or to spectral variations.

Table II. Full list of calculated degradation rates.

	Based on archived data: monitoring period 2003–2008 range					Recent field measurements (2010–2011)
Sub-Array	P_{MP-ARC} (%/year)	Monthly PR_{DC} (%/year)	Monthly PR_{AC} (%/year)	15-min PR_{DC} (%/year)	15-min PR_{AC} (%/year)	*I-V* compared with initial data (%/year)
MMS 1	-0.84 ± 0.014	-0.8 ± 0.33	-0.9 ± 0.35	-0.80 ± 0.021	-1.02 ± 0.021	-1.8 ± 1.6
MMS 2	-0.99 ± 0.013	-0.9 ± 0.35	-1.0 ± 0.36	-0.95 ± 0.021	-0.88 ± 0.022	-1.8 ± 1.7
CEL 1	-1.47 ± 0.058	-0.8 ± 0.88	-0.7 ± 0.93	-1.39 ± 0.058	-1.27 ± 0.058	-2.7 ± 1.2
CEL 2	-1.23 ± 0.059	-0.6 ± 0.87	-0.5 ± 0.92	-1.16 ± 0.057	-1.08 ± 0.056	-2.2 ± 1.3
CEL 1(uncorrected)	-3.45[a]	—	—	—	—	—
CEL 2(uncorrected)	-3.23[a]	—	—	—	—	—

[a]Because of large systematic error because of sensor drift, uncertainty values are not reported here.
MMS, Meigs Middle School; CEL, Celebration School.

sub-array 2. For CEL, sub-array 1 was -1.47 ± 0.058%/year and sub-array 2 was -1.23 ± 0.059%/year.

3.2. Degradation rates based on PR_{DC} and PR_{AC}

Figure 6 shows the monthly AC and DC PRs for both systems. Because PR is inversely proportional to the incident solar energy, an upward drift in irradiance data from the uncalibrated pyranometer at CEL would have obviously affected the degradation rate if the data had not been corrected, making it appear higher than it actually is.

Performing a linear regression on the monthly PR values (using the same filtering as described previously), the calculated DC and AC degradation rates were found to be in good agreement for all of the individual sub-arrays. The DC degradation rate for MMS sub-array 1 was found to be -0.8 ± 0.33%/year and -0.9 ± 0.35%/year on the AC side. MMS sub-array 2 had a -0.9 ± 0.35%/year DC degradation rate and -1.0 ± 0.36%/year on the AC side. The CEL system showed similar agreement, with sub-array 1 having a -0.8 ± 0.88%/year DC degradation and -0.7 ± 0.93%/year AC degradation. For CEL sub-array 2, a -0.6 ± 0.87%/year DC degradation was calculated and -0.5 ± 0.92%/year AC degradation rate.

The large discrepancy between ΔR_d for P_{MP-ARC} as compared with PR_{DC} and PR_{AC} is likely due to the fact that the P_{MP-ARC} is based on 15-min averages and the regression therefore has 35 040 data points per year. PR, on the other hand, is calculated using only 12 data points per year (monthly increments). Upon recalculating PR_{DC} and PR_{AC} using 15-min increments as opposed to a monthly basis, the values for R_d and ΔR_d were found to be much closer to those calculated from P_{MP-ARC}.

The larger uncertainty values for CEL, as compared with MMS, are due to the shorter monitoring period. This has been shown to be the case in past studies as well [14], and it makes sense intuitively, because less monitoring time would likely mean less certainty in establishing a clear degradation trend.

3.3. Field observations and on-site measurements

Upon visiting both sites, a thorough visual inspection was performed, followed by thermal imaging analysis using an infrared camera [25] and *I-V* measurements using a

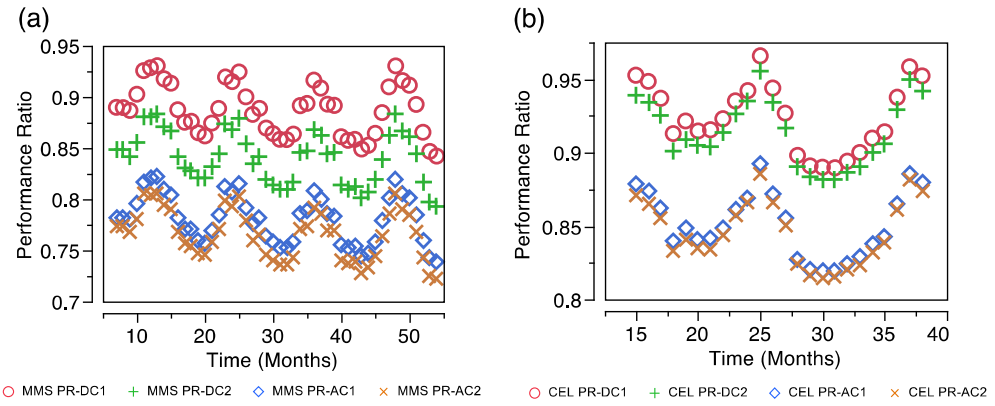

Figure 6. Performance Ratio (PR) calculated for sub-arrays (PR_{DC}) and sub-systems (PR_{AC}) for: (a) Meigs Middle School (MMS) data set, (b) irradiance-corrected Celebration School (CEL) data set.

portable curve tracer (Daystar DS-100). On the basis of the visual inspections, multiple issues were found, including one inverter failure at MMS, the coastal site. There were also concerns regarding corrosion of the grounding hardware for both systems (Figure 7(a) and (b)), as well as mounting hardware corrosion at MMS. As a side note, there was some very light soiling because of dust and pollen on both systems (inspections were performed during spring in both cases), but this was concentrated at the bottom of the modules, not shading any cells directly. A few modules had some stains in the front glass. Still, these defects did not result in any significant changes that could separate these from the other modules.

In regards to the thermal imaging, a hotspot was found on one of the polycrystalline-Si cells at the CEL site (Figure 7(c)). The digital photograph in Figure 7(d) features a digital photograph of that same cell, which shows apparent melting of the contact fingers at the hottest points on the cell. As expected, this sub-array showed the most drastic reduction in performance of all four sub-arrays. It should be noted that if there were hotspots on the MMS sub-array connected to the failed inverter, those hotspots may not have shown up because the array was not loaded (open-circuit condition).

I-V curves were taken on all four sub-arrays (two at MMS and two at CEL). The same portable curve tracer was used for both systems, and calibrated pyranometers were brought on-site to measure POA irradiance. To measure module back-surface temperature, the existing thermocouples at both sites were rewired from the datalogger instrument panel to the curve tracer. These thermocouples were inspected to ensure they were still properly adhered to the back of the modules. Figure 8(a) shows a single representative *I-V* curve for all four sub-arrays. Multiple *I-V* measurements were made for each sub-array (7 curves for MMS 1, 9 for MMS 2, 13 for CEL 1, 15 for CEL 2) and the P_{MP} values extracted from these have been translated to ARC using Equations 1–3. The average P_{MP-ARC} values are included in Table III.

As a point of comparison, the initial ARC-translated power output for the arrays has been included (Figure 8(b)). This initial power output was determined from the archived data set as described in the previous section and was taken as the mean of the ARC-translated power during the first available month of data collection that coincided with the same month in which the on-site measurements were performed (to avoid seasonal effects). In all four cases, the standard deviation fell well within the ± 70 W uncertainty given, which was calculated using the familiar uncertainty propagation equation for P_{MP-ARC} knowing the key uncertainty contributors (e.g., irradiance measurement/translation, temperature measurement/translation, curve tracer accuracy).

The resulting degradation rates based on the *I-V* curve measurements were somewhat higher than those calculated from the archived data for all four sub-arrays and especially higher for CEL 1. For both MMS sub-array 1 and 2, R_d was found to be $-1.8 \pm 1.6\%$/year and $-1.8 \pm 1.7\%$/year, respectively. The CEL degradation rates were found to be higher, with $-2.7 \pm 1.2\%$/year for sub-array 1 (hotspot) and $-2.2 \pm 1.3\%$/year for sub-array 2. The source of these higher degradation rates is difficult to identify because of a lack of maintenance records by the system owners. It is possible that significant downtimes

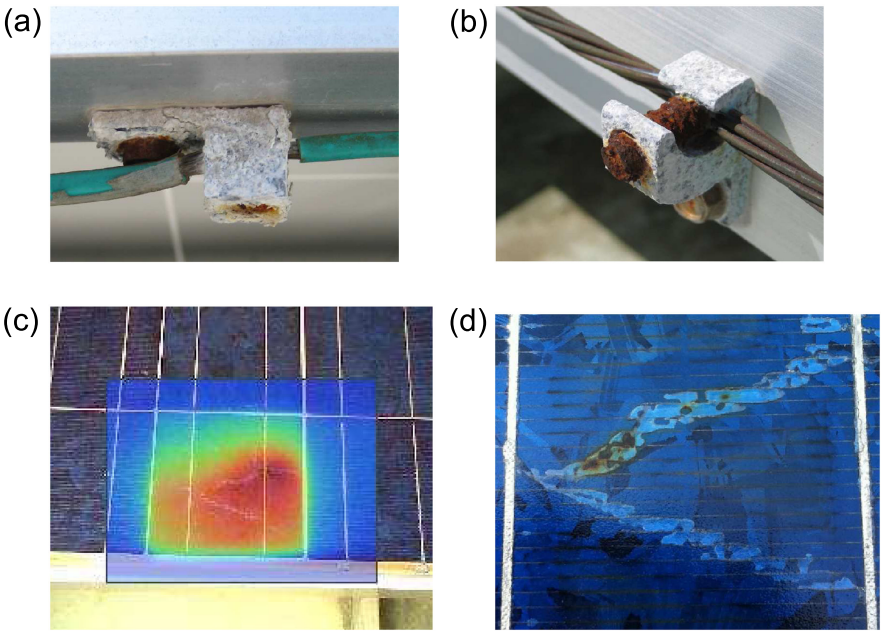

Figure 7. Pictures of systems: (a) corroded grounding lugs at Meigs Middle School site, (b) corroded grounding lugs at CEL site, (c) infrared image of hotspot on Celebration School system, (d) digital photograph of that same hotspot.

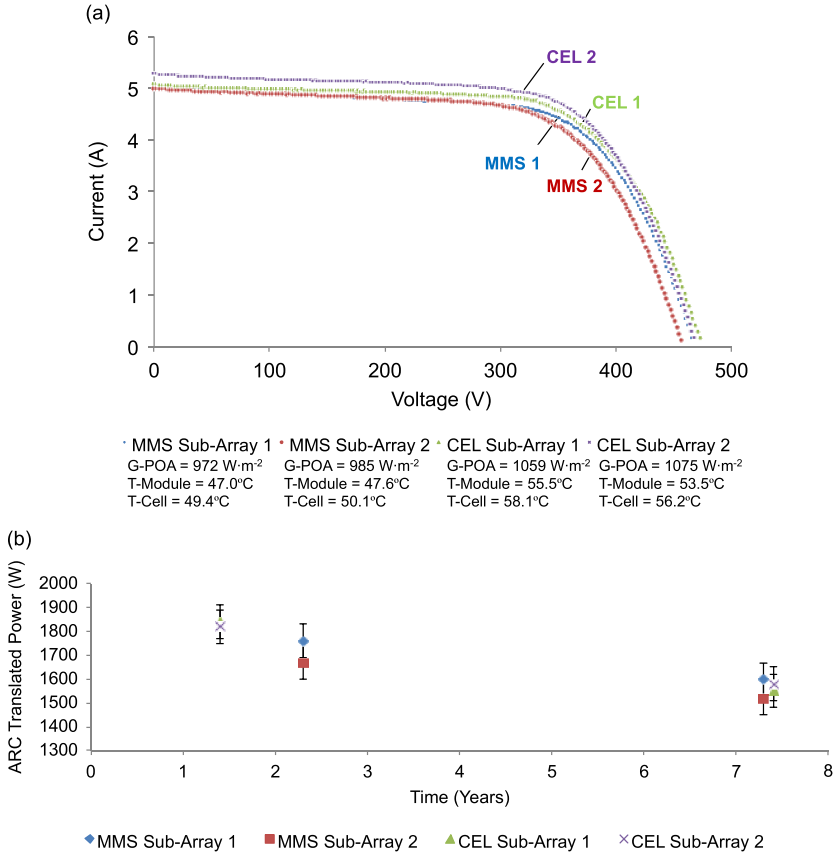

Figure 8. (a) Field *I-V* measurements performed on both systems, (b) alternative reporting condition (ARC)-translated power output based on initial power output from archived data and recent field measurements.

Table III. Comparison of the average ARC-translated power output values measured on-site (12 series connected modules per sub-array) and the nameplate rated STC power.

Power rating(all in watts)	MMSSub-array 1	MMSSub-array 2	CELSub-array 1	CELSub-array 2
Array nameplate at STC (W)	1980	1980	1980	1980
Initial measured output at ARC (W)	1790 ± 70	1710 ± 70	1850 ± 70	1820 ± 70
•MMS May 2005				
•CEL April 2005				
Measured on-site power of field-aged modules translated to ARC (W)	1600 ± 70	1520 ± 70	1550 ± 70	1580 ± 70
•MMS 18 May 2010				
•CEL 27 April 2011				

ARC, alternative reporting condition; STC, Standard Test Conditions; MMS, Meigs Middle School; CEL, Celebration School.

because of inverter failure or other problems could have accelerated the degradation [15]. Whatever the cause, any degradation would only be compounded by the fact that the modules in each sub-array are series connected, and mismatch because of one module would thereby affect the entire string. In addition, the high uncertainty in these calculations must also be considered, and the fact that the power values used at the two different points in time were measured with different instrumentation, including different pyranometers.

4. CONCLUSION

After reviewing the archived data for both systems under investigation (MMS and CEL), it became clear that the pyranometer used for the CEL system had noticeable sensor drift. The MMS system, on the other hand, proved to have high-quality irradiance data with no obvious correction required. After describing the irradiance correction technique and results, a description of the analytical techniques used to establish degradation rates was then given

(power output translated to ARC, PR). Using results of the techniques described in this paper, degradation rates were established for both systems and are summarized in Table II. For the archived data used in this study, the degradation rates were all in the range of $-1 \pm 1\%$/year. Although these calculated degradation rates are slightly higher than the average value reported for c-Si modules by a recent review article (-0.7%/year), values larger than -1% per year have been reported [17]. This is understandable considering the additional array and system-level losses that can increase degradation, as compared with module-level studies. On-site measurements of *I-V* characteristics were performed on both systems. The measured P_{MP} values were translated to ARC and compared with the initial archived data. These resulting degradation rates were found to be a little higher than expected for MMS 1, MMS 2, and CEL 2, and very significantly higher for CEL 1, which is likely due to the presence of a hotspot. These higher levels of degradation, occurring after the monitoring period listed in Table I could be due to improper operation of the arrays (e.g., significant inverter downtime) or perhaps because of the large uncertainty associated with them. A lack of maintenance records makes this challenging to determine.

Uncertainty calculations were performed on the degradation rates using a simple Type A evaluation. This method does not account for systematic uncertainties that are induced by drift in the irradiance sensors. This systematic error has been addressed by the aforementioned irradiance correction technique, but it is quite possible that the systematic uncertainty still outweighs the random uncertainty calculated in this study. A comparison of degradation rates calculated by the raw data (with apparent drift) and irradiance-corrected data resulted in a 2%/year difference in the degradation rates for both sub-arrays. This difference dwarfs the random uncertainty calculated via a Type A evaluation, which suggests that one of the biggest challenges in accurately determining degradation rates using field data is due to irradiance sensor drift and calibration requirements. It is clear that more stable irradiance sensors, at a reasonable cost and with minimal calibration requirements, would be quite valuable in efforts to determine the degradation rates of deployed PV systems [26].

The multi-pronged approach that has been introduced provides a means of evaluating performance over extended periods of time, which can (i) help identify reliability concerns, (ii) account for seasonal variations, and (iii) quantify module degradation. All three of these points are pertinent to system owners, especially at the utility scale where time of generation becomes a factor.

Future efforts will be oriented toward applying this method to a significantly larger sample of systems in the FSEC PV system database to gain statistical information on module durability in hot, humid climates. In addition, performing *I-V* measurements on individual modules within fielded arrays will be important in better understanding the influence of mismatch over time.

ACKNOWLEDGEMENTS

The authors would like to acknowledge the many researchers that spent time installing and maintaining the FSEC PV system database, including William Wilson, Stephen Barkaszi, Donard Metzger, Jim Dunlop, and Kevin Lynn, as well as the Florida Automated Weather Network at the University of Florida for providing public access to high-quality environmental data. The authors would also like to acknowledge NREL for funding this research effort through subcontract number NFE99901501. This work was supported by the U.S. Department of Energy under Contract No. DE-AC36-08-GO28308 with the National Renewable Energy Laboratory.

REFERENCES

1. Parker DS, Dunlop JP, Barkaszi SF, Sherwin JR, Anello MT, Sonne JK. Towards zero energy demand: evaluation of super efficient building technology with photovoltaic power for new residential housing. *Proceedings of the 2000 ACEEE Summer Study on Energy Efficiency in Buildings*, Vol. **1**. American Council for an Energy Efficient Economy: Washington, DC, 2000; 214.
2. Parker DS. Very low energy homes in the United States: perspectives on performance from measured data. *Energy and Buildings* 2009; **41**: 512–520. doi: 10.1016/j.enbuild.2008.11.017.
3. Lynn K, Szaro J, Wilson W, Healey M. A review of PV system performance and life-cycle costs for the Sunsmart schools program. *Proc. of the ASME International Solar Energy Conference* 2006, Denver, CO; 153–156.
4. Davis K, Moaveni H. Effects of module performance and long-term degradation on economics and energy payback: case study of two different photovoltaic technologies. *Proceedings of the Society of Photo-Optical Instrumentation Engineers (SPIE) 7412* 2009, 74120Y, San Diego, CA. doi: 10.1117/12.830097.
5. Osterwald CR, Adelstein J, del Cueto JA, Kroposki B, Trudell D, Moriarty T. Comparison of degradation rates of individual modules held at maximum power. *Proceedings of the 4th World Conference on Photovoltaic Energy Conversion*, Waikoloa, HI, 2006; 2085–2088. doi: 10.1109/WCPEC.2006.279914.
6. Vázquez M, Rey-Stolle I. Photovoltaic module reliability model based on field degradation studies. *Progress in Photovoltaics: Research and Applications* 2008; **16**: 419–433. doi: 10.1002/pip.825.
7. King DL, Quintana MA, Kratochvil JA, Ellibee DE, Hansen BR. Photovoltaic module performance and durability following long-term exposure. *Progress in*

Photovoltaics: Research and Application 2000; **8**: 241–256.
8. Quintana MA, King DL, Hosking FM, et al. Diagnostic analysis of silicon photovoltaic modules after 20-year field exposure. *Proceedings of the 28th PV Specialists Conference*, Anchorage, AK, USA, 2000; 1420–1423. doi: 10.1109/PVSC.2000.916159.
9. Reis AM, Coleman NT, Marshall MW, Lehman PA, Chamberlin, CE. Comparison of PV module performance before and after 11-years of field exposure. *Proceedings of the 29th PV Specialists Conference*, New Orleans, LA, USA, 2002; 1432–1435. doi 10.1109/PVSC.2002.1190878.
10. Carr AJ, Pryor TL. A comparison of the performance of different PV module types in temperate climates. *Solar Energy* 2004; **76**: 285–294. doi:10.1016/j.solener.2003.07.026.
11. Wohlgemuth JH, Cunningham DW, Nguyen AM, Miller J. Long term reliability of PV modules. *Proceedings of the 20th European Photovoltaic Solar Energy Conference*, Barcelona, Spain, 2005; 1942–1948.
12. Cereghetti N, Burà E, Chianesse D, Friesen G, Realini A, Rezzonico S. Power and energy production of PV modules statistical considerations of 10 years of activity. *Proceedings of the 3rd Conference on Photovoltaic Energy Conversion*, Osaka, Japan, 2003; 1919–1922.
13. Skoczek A, Sample T, Dunlop ED. The results of performance measurements of field-aged crystalline silicon photovoltaic modules. *Progress in Photovoltaics: Research and Application* 2009; **17**: 227–240. doi: 10.1002/pip.874.
14. Jordan DC, Smith RM, Osterwald CR, Gelak E, Kurtz SR. Outdoor PV degradation comparison. *Proceedings of the 35th IEEE PV Specialist Conference*, Honolulu, HI, USA, 2010; 2694–2697. doi: 10.1109/PVSC.2010.5616925.
15. Abenante L, De Lia F, Castello S. Long-term performance degradation of c-Si photovoltaic modules and strings. *Proceedings of 25th European Photovoltaic Solar Energy Conference*, Valencia, Spain, 2010; 4023–4026. doi: 10.4229/25thEUPVSEC2010-4AV.3.19.
16. Ishii T, Takashima T, Otani K. Long-term performance degradation of various kinds of photovoltaic modules under moderate climatic conditions. *Progress in Photovoltaics: Research and Applications* 2011; **19**: 170–179. doi: 10.1002/pip.1005.
17. Jordan DC, Kurtz SR. PV degradation rates—an analytical review. submitted to *Progress in Photovoltaics: Research and Applications*.
18. International Electrotechnical Commission, *IEC 61724 Ed. 1.0*.
19. King DL, Boyson WE, Kratochvil JA. Photovoltaic array performance model. SAND2004-3535, 2004.
20. Whitfield K, Osterwald CR. Procedure for determining the uncertainty of photovoltaic module outdoor electrical performance. *Progress in Photovoltaics: Research and Applications* 2001; **9**: 87–102. doi: 10.1002/pip.356.
21. King DL, Kratochvil JA, Boyson WE, Bower W. Field experience with a new performance characterization procedure for photovoltaic arrays. *Proceedings of the 2nd World Conference and Exhibition on Photovoltaic Solar Energy Conversion*, Vienna, Austria, 1998; 1947–1952.
22. Marion B, Adelstein J, Boyle K, et al. Performance parameters for grid-connected PV systems. *Proceedings of the 31st IEEE Photovoltaic Specialist Conference*, Orlando, FL, 2005; 1601–1606. doi: 10.1109/PVSC.2005.1488451.
23. ISO Guide to the Expression of Uncertainty in Measurement or GUM. 1995. The U.S. edition of the GUM is entitled: American National Standard for Expressing Uncertainty—U.S. Guide to the Expression of Uncertainty in Measurement, ANSI/NCSL Z540-2-1997.
24. Drosg M. *Dealing with Uncertainties: A Guide to Error Analysis* (2nd edn). Springer-Verlag: Berlin Heidelberg, 2009.
25. King DL, Kratochvil JA, Quintana MA, McMahon TJ. Applications for infrared imaging equipment in photovoltaic cell, module, and system testing. *Proceedings of the 28th IEEE Photovoltaic Specialist Conference*, Anchorage, AK, 2000; 1487–1490. doi: 10.1109/PVSC.2000.916175.
26. Cronin A, Pulver S, Cormode D, Jordan D, Kurtz S, Smith R. Measuring degradation rates without irradiance data. submitted to *Progress in Photovoltaics: Research and Applications*.